

Titanium oxide Nanoparticles: Analysis and Photodegradation activity for Hexamethylpararosaniline chloride

Dhuha H. Fadhil

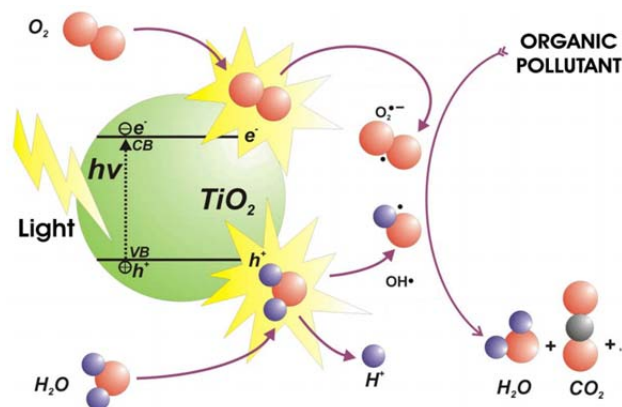
Department of Chemistry, College of Science,
Al-Nahrain University, Baghdad, Iraq

Abstract

Titanium oxide Nanoparticles has been synthesized regarding to Sol-Gel technique. Sized and morphology of Titanium oxide Nanoparticles had been investigated based on X-ray diffraction in addition to, scanning electron microscope. Photodegradation of dye named hexamethylpararosaniline chloride was done under UV light illumination using Titanium oxide Nanoparticles. The impact of concentrations, pH and irradiation time for Titanium Oxide Nanoparticles with hexamethylpararosaniline chloride was investigated. The results exhibited that the denaturation of hexamethylpararosaniline chloride had been done with good activity.

INTRODUCTION

Dyes have a significant origin of ecological pollution. Fabric wastewater include generally a huge amount of un-fixed dyes, numerous of them were azo-dyes [1]. It has evaluated that 15% of all dyes manufactures are wasted through dyes approach and it was released in water [2]. The hues created by moment measures of colors inadvertently discharged in water amid kicking the bucket procedures are considered to posture significant issues, since they have impressive natural impacts on the water and make them outwardly unsavory [3]. In addition, natural contamination by natural colors additionally sets an extreme biological issue, which is expanded by the way that the vast majority of them are frequently poisonous to microorganisms and a have long corruption times in the earth [4]. Semiconductor photocatalysis by TiO_2 has been broadly studied for a long time. Potential uses incorporate devastation of microscopic organisms [5], the oxidation of toxins [6], e.g., color buildups [7], and expulsion of natural movies from glass and polymer substrates [8]. In any case, early work stressed undesirable perspectives, e.g., photocatalytic corruption of TiO_2 pigmented paint movies [9] or material strands [10]. Business research to minimize TiO_2 photocatalysis proceeds, yet little is distributed in the open writing. Both destinations have driven research into the photocatalytic instrument [11,12]. Vast energy-gap semi-conductor such as titanium oxide are usually explored with energy gap 3.0 electron volt and energy gap 3.2 electron volt, stages and titanium oxide promoted to ultraviolet was not only led to photo-catalysis research [13–15] and as well as to prod examination of titanium oxide ultra-hydro-philicity its utilization in ecological treatment with sun power fuel generation. Energy-gap excitation of titanium oxide issue charge segregation obeyed via electrons scavenging in addition to holes through adsorbing surface type, as in Scheme 1:



Scheme 1. Graphical of semi-conductor excited through energy gap enlightenment [16] major to electrons induction in band of conduction with the valence band holes.

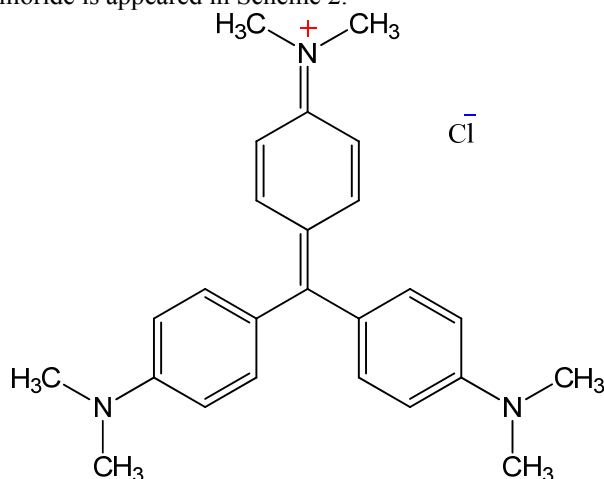
One imperative reason that thwarts the comprehension of the instruments is the unpredictability of the photocatalytic procedure. In the photocatalytic response, the h^+vb -incited oxidation half response and the e^-cb -actuated lessening half response continue on the surface of one photocatalyst molecule (as a rule of a nano measure) in the meantime, which makes it hard to recognize them in space and time. Also, the photocatalytic response includes a progression of dynamic free radical species and procedures. It is trying to research these species and procedures with consistent state methods. The isotopic marking strategy is a standout amongst the most intense procedures to disentangle confused response instruments [17]. Stable isotope checking, particularly by $^{13}\text{C}/^{12}\text{C}$, $\text{H}/(\text{D} = 2 \text{ H})$ and $^{18}\text{O}/^{16}\text{O}$, is an adaptable diagnostic instrument crosswise over numerous domains of science [18]. In the TiO_2 photocatalytic framework, the principle response segments O_2 , H_2O and TiO_2 all contain oxygen molecules. As needs be, oxygen isotope naming can be the most immediate and dependable technique to follow the O-molecule starting

point of items and recognize the part and pathways of these segments in the diverse photocatalytic responses. Another preferred standpoint of oxygen isotopic naming strategy is its adaptability, i.e., every segment, for example, ^{18}O -marked $^{18}\text{O}_2$ [19–23], H_2 ^{18}O [24–26], Ti_{18}O_2 [27–32] and ^{18}O -named substrate [33–35] can be named. On the TiO_2 surface, the ^{18}O -marked strategy has been often utilized as a part of oxygen isotopic trade estimations to concentrate the dependability of surface oxygen in thermally enacted synergist responses [36,37]. All the more regularly, this technique was utilized in gas stage TiO_2 photocatalytic frameworks to research the photoinduced oxygen isotopic trade with the point of comprehension the advancement of the middle of the road species on the TiO_2 surface [38–45]. The point of the present work was to research the impact of different parameters on the photocatalytic corruption of colors, in particular hexamethylpararosaniline chloride, by UV-light illumination within the sight of TiO_2 .

EXPERIMENTAL METHODS

Reagents and Materials

Hexamethylpararosaniline chloride colors an every other reagent were bought from Sigma-Aldrich and were utilized as received from the provider with no further sanitization. The substance structure of the hexamethylpararosaniline chloride is appeared in Scheme 2.



Scheme 2: The chemical structure of the studied dye hexamethylpararosaniline chloride

Synthesis of TiO_2

TiO_2 nano-materials were readied by means of sol-gel technique utilizing titanium tetraisopropoxide, refined water, ethyl liquor and hydrochloric corrosive as the beginning materials. Focuses with volume proportion of titanium tetraisopropoxide; ethanol, water and hydrochloric corrosive 1:15:60:0.2 respectively. Titanium tetraisopropoxide was dropped gradually into the arrangement of water, liquor and corrosive while attractive fomenting consistently to get white slurry arrangement. The acquired arrangements were kept under moderate speed consistent mixing on an attractive stirrer for 48 h at room temperature. At that point the accelerated TiO_2 was separated and dried at 50°C for 2 h until it was transformed into white piece precious stone. After ball processing the

dried powders acquired were calcinated at 400 and 900°C for 3 h to watch the stage changes going with the warmth medications.

Techniques

The photograph reactor comprises of lights as UV light source centrifuged to expel the suspended impetus particles. The supernatant hexamethylpararosaniline chloride arrangements were broke down by UV-obvious spectrophotometer for the assurance of grouping of the rest of the color. Absorbance's of the color arrangements were measured at the λ_{max} of hexamethylpararosaniline chloride color at 519 nm. From the estimations of absorbance, the centralization of color was computed from the standard adjustment bend. ($\lambda_{\text{max}} = 365$ nm). The readied color arrangements hexamethylpararosaniline chloride was taken in UV-light photoreactor. The required sum (0.020 g) of blended TiO_2 was added to the above color arrangement. Before light the hexamethylpararosaniline chloride arrangements were kept under dull condition for 30 min. At that point it kept inside UV light photoreactor for 75 min. The gathered suspension was centrifuged and separated before the UV-noticeable assimilation estimations. The corruption rate of both colors were evaluated by the accompanying condition,

$$\text{Percentage removal (\% R)} = 1 - \frac{C_1}{C_2}$$

where, C_1 & C_2 is the initial & final concentration of Hexamethylpararosaniline (ppm) at a given time

SEM images

The surface morphology of the calcinated powders at 400°C was seen on a filtering electron microscopy (SEM). Morphology of the nanoparticles was examined by, Scanning electron spectroscopy instrument, Phillips, show XL30

Powder X-beam diffraction

XRD was utilized for recognizable proof of crystalline stages and estimation of the crystallite measure. From the line expanding of comparing X-beam diffraction pinnacles and utilizing the Scherrer equation the crystallite measure, L has been evaluated [46]. $L = K\lambda/(\beta \cos \theta)$ where λ is the wavelength of the X-beam radiation, K is a consistent, β is the line width at half most extreme tallness, and θ is the diffracting edge.

RESULTS AND DISCUSSION

Impact of Concentration of Dye

The photocatalytic decoloration of hexamethylpararosaniline chloride was done at various beginning focuses extending from 10 ppm to 50 ppm under UV light frameworks. The impact of centralization of hexamethylpararosaniline chloride builds the rate expulsion was reductions. Since more number of color atoms are adsorbed on the surface of the photocatalyst. So the photon entering pathway will be lessened. The corruption of hexamethylpararosaniline chloride as appeared in Figure 1, [47-48].

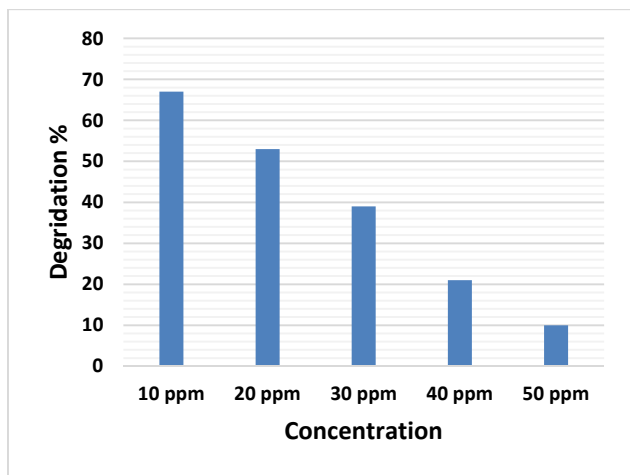


Figure 1: Effect of concentration of hexamethylparosaniline chloride.

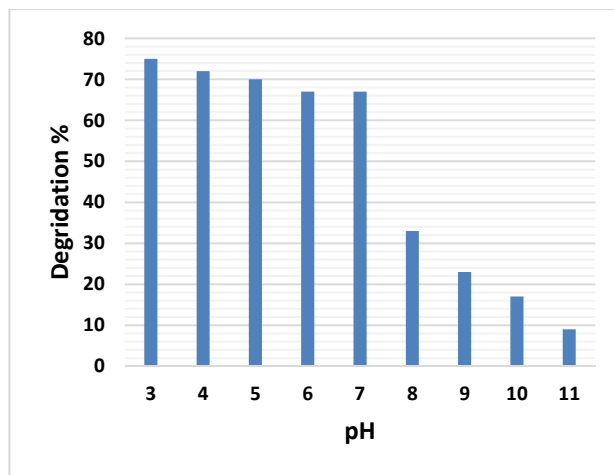


Figure 3. Effect of pH for hexamethylparosaniline chloride

Impact of Time variety

The rate of photodegradation increments with increment in light time and finish corruption was not gotten even following 180 minutes, but rather the vast majority of the hexamethylparosaniline chloride was evacuated after 80 min. hexamethylparosaniline chloride atoms and impetuses have enough time to participate in photocatalytic corruption handle and subsequently rate of debasement increments [49,50] as appeared in Figure 2.

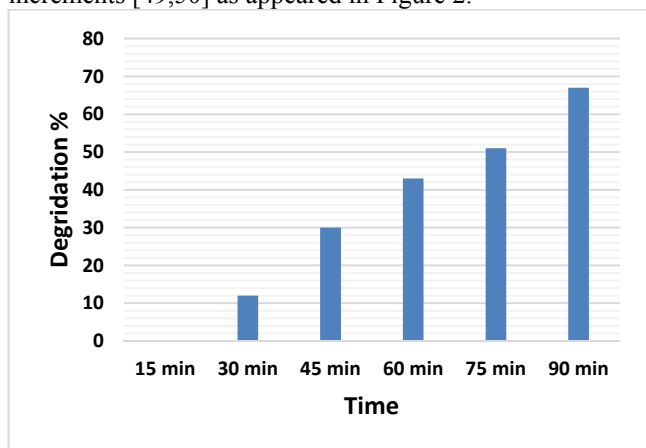


Figure 2: Time variation for hexamethylparosaniline chloride

Impact of pH

The impact of pH is one of the essential parameter for photodegradation of colors. Since it impacts the surface charge properties of the photocatalysts. The pH increments from 3 to 11. Along these lines, the hexamethylparosaniline chloride effectively pulled in by the contrarily charged impetus. The rate of corruption increments steadily with increment of pH [51] as appeared in Figure 3.

SEM

SEM pictures of the TiO₂ nanoparticles arranged by means of sol-gel are appeared in Figure 45. Figure 4, demonstrates the SEM picture of sol-gel inferred nanoparticles. Clear nanostructures can be seen has a normal size in the range 20nm. Checking Electron Microscopy perception indicated high homogeneity of the TiO₂ arranged by sol-gel technique.

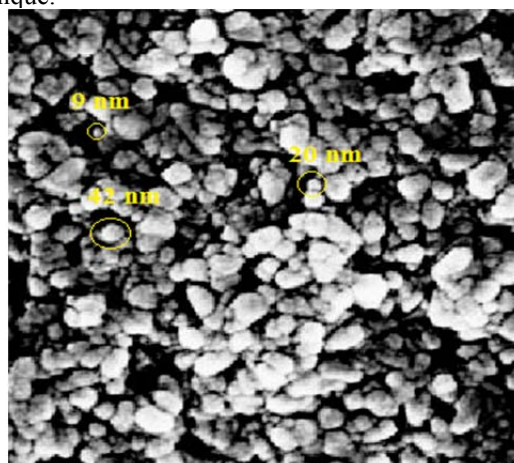


Figure 4, The SEM picture of TiO₂ nanoparticles

XRD

Figure 5, demonstrates the X-Ray Diffraction examples of orchestrated TiO₂ nanoparticles. From the line widening of comparing X-beam diffraction pinnacles and utilizing the Scherrer equation the crystallite measure, L has been assessed [46]. $L = K\lambda / (\beta \cos \theta)$ where λ is the wavelength of the X-beam radiation, K is a steady, β is the line width at half most extreme stature, and θ is the diffracting edge. The arranged TiO₂ nanoparticles X-Ray Diffraction designs demonstrated the nearness of expansive pinnacles. The wide pinnacles demonstrate either particles of little crystalline size, or particles are semi crystalline in nature.

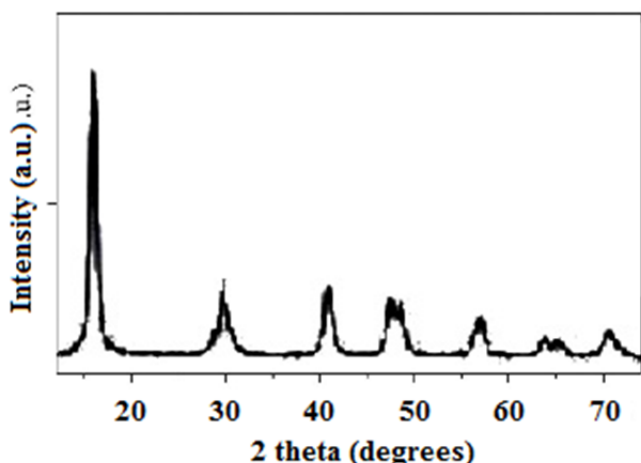


Figure 5, The XRD of TiO₂ nanoparticles

CONCLUSION

The TiO₂ nanoparticles were set up by sol gel technique. The consequences of SEM shows, the normal size of TiO₂ nanoparticles has a normal size in the range 20nm. The arranged TiO₂ nanoparticles X-Ray Diffraction designs demonstrated the nearness of wide pinnacles. The expansive pinnacles demonstrate either particles of little crystalline size, or particles are semi crystalline in nature. The natural color hexamethylpararosaniline chloride was effectively corrupted by the arranged TiO₂ nanoparticles under light UV illumination. The blended TiO₂ nanoparticles could be utilized for expulsion of hexamethylpararosaniline chloride as waste water which adds to the ecological contamination.

REFERENCES

- Chen, C.; Wang, Z.; Ruan, S.; Zou, B.; Zhao, M.; Wu, F. Photocatalytic degradation of C.I. Acid Orange 52 in the presence of Zn-doped TiO₂ prepared by a stearic acid gel method. *Dyes Pigm.* 2008, 77, 204-209.
- Vautier, M.; Guillard, C.; Herrmann, J. Photocatalytic Degradation of Dyes in Water: Case Study of Indigo and of Indigo Carmine. *J. Catal.* 2001, 201, 46-59.
- Wang, C.; Lee, C.; Lyu, M.; Juang, L. Photocatalytic degradation of C.I. Basic Violet 10 using TiO₂ catalysts supported by Y zeolite: An investigation of the effects of operational parameters. *Dyes Pigm.* 2008, 76, 817-824.
- Zainal, Z.; Hui, L.K.; Hussein, M.Z.; Taufiq-Yap, Y.H.; Abdullah, A.H.; Ramli, I. Removal of dyes using immobilized titanium dioxide illuminated by fluorescent lamps. *J. Hazard. Mater.* 2005, 125, 113-120.
- Matsunaga, T.; Okochi, M. TiO₂ Mediated Photochemical Disinfection of Escherichia coli Using Optical Fibers. *Environ. Sci. Technol.* 1995, 29, 501-505.
- Maillard, C.; Guillard, C.; Pichat, P. Comparative effects of the TiO₂-UV, H₂O₂-UV H₂O₂-Fe²⁺ systems on The disappearance Rate of benzamide and 4-hydroxybenzamide in water. *Chemosphere* 1992, 24, 1085-1094.
- Mills, A.; Belghazi, A.; Davies, R.H.; Morris, S.A. Kinetic study of the bleaching of Rhodamine 6G photosensitized by titanium dioxide. *J. Photochem. Photobiol. A* 1994, 79, 131-139
- Fateh, R.; Dillert, R.; Bahnemann, D. Self-cleaning properties, mechanical stability, and adhesion strength of transparent photocatalytic TiO₂-ZnO coatings on polycarbonate. *ACS Appl. Mater. Interfaces* 2014, 6, 2269-2277.
- Hughes, W. Phodegradation of paint films containing TiO₂ pigments. In *Xth FATIPEC Congress 1970*; Verlag Chemie GmbH: Weinheim/Bergst, Germany, 1970; pp. 67-82.
- Allen, N.S.; McKellar, J.F.; Phillips, G.O.; Chapman, C.B. The TiO₂ photosensitized degradation of nylon 6, 6: Stabilizing action of manganese ions. *J. Polym. Sci. C Polym. Lett.* 1974, 12, 723-727.
- Yousif E, Abdalla M., Ahmed A., Salimon J., Salih N., Photochemical stability and photostabilizing efficiency of poly(methyl methacrylate) based on 2-thioacetic acid-5-phenyl-1,3,4-oxadiazole complexes, *Arabian Journal of Chemistry* 9(2016) S595-S601.
- Egerton, T.A.; King, C.J. The Influence of Light Intensity on Photoactivity in TiO₂ pigmented systems. *J. Oil Colour Chem. Assoc.* 1979, 62, 386-391
- Ibhadon, A.O. Multifunctional TiO₂ Catalysis and Applications. In *Proceedings of Green Chemistry and Engineering International Conference*, Washington, DC, USA, 24-26 June 2008.
- Sodis Water Project. Available online: <http://cordis.europa.eu/documents/documentlibrary/122807461EN6.pdf> (accessed on 20 February 2013).
- Cho, M.; Chung, H.; Choi, W.; Yoon, J. Linear correlation between inactivation of E. coli and OH radical concentration in TiO₂ photocatalytic disinfection. *Water Res.* 2004, 38, 1069-1077.
- Fujishima, A.; Zhang, X.; Tryk, D.A. TiO₂ photocatalysis and related surface phenomena. *Surf. Sci. Rep.* 2008, 63, 515-582.
- Holmes, J.L.; Jobst, K.J.; Terlouw, J.K. Isotopic labelling in mass spectrometry as a tool for studying reaction mechanisms of ion dissociations. *J. Label. Compd. Radiopharm.* 2007, 50, 1115-1123.
- Lloyd-Jones, G.C.; Munoz, M.P. Isotopic labelling in the study of organic and organometallic mechanism and structure: An account. *J. Label. Compd. Radiopharm.* 2007, 50, 1072-1087.
- Almeida, A.R.; Moulajn, J.A.; Mul, G. Photocatalytic oxidation of cyclohexane over TiO₂: Evidence for a Mars-van Krevelen mechanism. *J. Phys. Chem. C* 2011, 115, 1330-1338.
- Epling, W.S.; Peden, C.H.F.; Henderson, M.A.; Diebold, U. Evidence for oxygen adatoms on TiO₂ (110) resulting from O₂ dissociation at vacancy sites. *Surf. Sci.* 1998, 412-413, 333-343.
- Kim, H.H.; Ogata, A.; Schiorlin, M.; Marotta, E.; Paradisi, C. Oxygen isotope (O-18(2)) evidence on the role of oxygen in the plasma-driven catalysis of VOC oxidation. *Catal. Lett.* 2011, 141, 277-282.
- Liao, L.F.; Lien, C.F.; Shieh, D.L.; Chen, M.T.; Lin, J.L. Ftir study of adsorption and photoassisted oxygen isotopic exchange of carbon monoxide, carbon dioxide, carbonate, and formate on TiO₂. *J. Phys. Chem. B* 2002, 106, 11240-11245.
- Thompson, T.L.; Diwald, O.; Yates, J.T. Molecular oxygen-mediated vacancy diffusion on TiO₂ (110)—new studies of the proposed mechanism. *Chem. Phys. Lett.* 2004, 393, 28-30.
- Wu, T.P.; Kaden, W.E.; Anderson, S.L. Water on rutile TiO₂ (110) and Au/ TiO₂ (110): Effects on a mobility and the isotope exchange reaction. *J. Phys. Chem. C* 2008, 112, 9006-9015.
- Suprun, W.; Sadovskaya, E.M.; Rudinger, C.; Eberle, H.J.; Lutecki, M.; Papp, H. Effect of water on oxidative scission of 1-butene to acetic acid over V₂O₅-TiO₂ catalyst. Transient isotopic and kinetic study. *Appl. Catal. A Gen.* 2011, 391, 125-136.
- Bui, T.D.; Yagi, E.; Harada, T.; Ikeda, S.; Matsunura, M. Isotope tracing study on oxidation of water on photoirradiated TiO₂ particles. *Appl. Catal. B Environ.* 2012, 126, 86-89.
- Civis, S.; Ferus, M.; Kubat, P.; Zukalova, M.; Kavan, L. Oxygen-isotope exchange between CO₂ and solid (TiO₂)-O-18. *J. Phys. Chem. C* 2011, 115, 11156-11162.
- Montoya, J.F.; Ivanova, I.; Dillert, R.; Bahnemann, D.W.; Salvador, P.; Peral, J. Catalytic role of surface oxygens in TiO₂ photooxidation reactions: Aqueous benzene photooxidation with (TiO₂)-O-18 under anaerobic conditions. *J. Phys. Chem. Lett.* 2013, 4, 1415-1422.
- Frank, O.; Zukalova, M.; Laskova, B.; Kurti, J.; Koltai, J.; Kavan, L. Raman spectra of titanium dioxide (anatase, rutile) with identified oxygen isotopes (16,17,18). *PCCP* 2012, 14, 14567-14572.
- Civis, S.; Ferus, M.; Zukalova, M.; Kavan, L.; Zelinger, Z. The application of high-resolution ir spectroscopy and isotope labeling for detailed investigation of TiO₂/gas interface reactions. *Opt. Mater.* 2013, 36, 159-162.
- Kavan, L.; Zukalova, M.; Ferus, M.; Kurti, J.; Koltai, J.; Civis, S. Oxygen-isotope labeled titania: Ti18O₂. *PCCP* 2011, 13, 11583-11586.
- Choi, J.; Kang, D.; Lee, K.H.; Lee, B.; Kim, K.J.; Hur, N.H. Evidence for light-induced oxygen exchange in the oxidation of

- liquid hydrocarbons on oxygen 18-labelled titanium dioxide. *RSC Adv.* 2013, 3, 9402–9407.
33. Li, X.J.; Jenks, W.S. Isotope studies of photocatalysis: Dual mechanisms in the conversion of anisole to phenol. *J. Am. Chem. Soc.* 2000, 122, 11864–11870.
 34. Zhang, X.G.; Ke, X.B.; Zheng, Z.F.; Liu, H.W.; Zhu, H.Y. TiO₂ nanofibers of different crystal phases for transesterification of alcohols with dimethyl carbonate. *Appl. Catal. B Environ.* 2014, 150, 330–337.
 35. Zhang, M.; Wang, Q.; Chen, C.C.; Zang, L.; Ma, W.H.; Zhao, J.C. Oxygen atom transfer in the photocatalytic oxidation of alcohols by TiO₂: Oxygen isotope studies. *Angew. Chem. Int. Ed.* 2009, 48, 6081–6084.
 36. Sato, S. Hydrogen and oxygen isotope exchange-reactions over illuminated and nonilluminated TiO₂. *J. Phys. Chem.* 1987, 91, 2895–2897.
 37. Yanagisawa, Y.; Sumimoto, T. Oxygen-exchange between CO₂ adsorbate and TiO₂ surfaces. *Appl. Phys. Lett.* 1994, 64, 3343–3344.
 38. Mikhaylov, R.V.; Lisachenko, A.A.; Titov, V.V. Investigation of photostimulated oxygen isotope exchange on TiO₂ Degussa P25 surface upon UV-Vis irradiation. *J. Phys. Chem. C* 2012, 116, 23332–23341.
 39. Avdeev, V.I.; Bedilo, A.F. Molecular mechanism of oxygen isotopic exchange over supported vanadium oxide catalyst VO_x/TiO₂. *J. Phys. Chem. C* 2013, 117, 2879–2887.
 40. Montoya, J.F.; Peral, J.; Salvador, P. Surface chemistry and interfacial charge-transfer mechanisms in photoinduced oxygen exchange at O₂- TiO₂ interfaces. *ChemPhysChem* 2011, 12, 901–907.
 41. Courbon, H.; Herrmann, J.M.; Pichat, P. Effect of platinum deposits on oxygen-adsorption and oxygen isotope exchange over variously pretreated, ultraviolet-illuminated powder TiO₂. *J. Phys. Chem.* 1984, 88, 5210–5214.
 42. Pichat, P.; Courbon, H.; Enriquez, R.; Tan, T.T.Y.; Amal, R. Light-induced isotopic exchange between O₂ and semiconductor oxides, a characterization method that deserves not to be overlooked. *Res. Chem. Intermed.* 2007, 33, 239–250.
 43. Avdeev, V.I.; Bedilo, A.F. Electronic structure of oxygen radicals on the surface of VO_x/TiO₂ catalysts and their role in oxygen isotopic exchange. *J. Phys. Chem. C* 2013, 117, 14701–14709.
 44. Sato, S.; Kadowaki, T.; Yamaguti, K. Photocatalytic oxygen isotopic exchange between oxygen molecule and the lattice oxygen of TiO₂ prepared from titanium hydroxide. *J. Phys. Chem.* 1984, 88, 2930–2931.
 45. Kumthekar, M.W.; Ozkan, U.S. Nitric oxide reduction with methane over Pd/TiO₂ catalysts. 2. Isotopic labeling studies using N-15, O-18, and C-13. *J. Catal.* 1997, 171, 54–66.
 46. Cullity B.D., *Elements of X-Ray Diffraction*, Adison 1978
 47. Devi L.G., Kumar S.G., Influence of physicochemical-electronic properties of transition metal ion doped polycrystalline titania on the photocatalytic degradation of Indigo Carmine and 4- nitrophenol under UV/solar light. *Appl. Surf. Sci.* 257 (2011) 2779-2790.
 48. Hoffmann M. R., Martin S. T., W. Choi W., Bahnemann D.W., Environmental applications of semiconductor photocatalysis, *Chem. Rev.* 95 (1995) 69-96.
 49. Meenakshi M., Sundaram M., Sangareswari P., Muthirulan, Enhanced photocatalytic activity of polypyrrole/TiO₂ nanocomposites for acid violet dye degradation under UV irradiation, *Int. J. Innov. Res. Sci. Eng.* (2014) 420-423.
 50. Wu S., Zheng H., Lian Y., Wu Y., Preparation, characterization and enhanced visible-light photocatalytic activities of BiPO₄/BiVO₄ composites, *Mater. Res. Bull.* 48 (2013) 2901-2907.
 51. Hussain Z., El-Hiti G.A., Ahmed A., N. Altaee, Yousif E., Photocatalytic Degradation of Polyhydroxybutyrate Films Using Titanium Dioxide Nanoparticles as a Photocatalys, *Russian Journal of Applied Chemistry*, 9 (2016). 1536–1543.